Nuclear relaxation and Overhauser effect in a nearly-one-dimensional Heisenberg system

J. P. Boucher, F. Ferrieu, and M. Nechtschein

Département de Recherche Fondamentale, Section de Résonance Magnétique, Centre d'Etudes Nucléaires de Grenoble, B.P. 85. Centre de Tri-38041, Grenoble-Cedex, France

(Received 16 July 1973)

The spin dynamics in a nearly-one-dimensional Heisenberg system—the solid free radical Tanol (2,2,6,6-tetramethyl-4-piperidinol-1-oxyl)—is studied through dynamical-nuclear-polarization (DNP) experiments (Overhauser effect) and proton spin-lattice relaxation-time (T_1) measurements. As the couplings between the electronic spins and the protons have been determined in Tanol, *absolute* determinations of the values of the electronic-spin-frequency correlation functions at the electronic Larmor frequency (ω_e) and at the nuclear Larmor frequency (ω_N) can be achieved by performing both DNP and T_1 measurements. The value obtained at ω_e is in agreement with theoretical calculations in one-dimensional Heisenberg systems using the method of Tahir-Kheli and McFadden. The value obtained at ω_N together with the frequency dependence of T_1 are explained by introducing a cutoff effect in the spin-diffusion process in one dimension. A derivation is given which expresses the magnitude of the cutoff effect in terms of the interchain couplings. An evaluation of the interchain couplings, using T_1 measurements, is presented. The values of the interchain couplings, which are consistent with both the T_1 measurements and the Néel temperature, are $J_1 \simeq J_2 \simeq 10^{-2}J$, where J is the intrachain exchange ($J/k = 4.1$ K), and J_1 and J_2 are the interchain couplings along two axis perpendicular to the chain. However, it cannot be excluded that, in Tanol, the disturbance of the spin-diffusion process is due to finite-length effects.

I. INTRODUCTION

Spin dynamics in one-dimensional Heisenberg systems described by the exchange Hamiltonian

$$E_c = -2J_0 \sum_i^{N-1} \vec{s}_i \cdot \vec{s}_{i+1} , \tag{1}$$

where J_0 is the exchange integral between nearest-neighbor spins s_i and s_{i+1}, have received considerable attention in recent years. The "motion" of the individual electronic spins can be studied through microscopic correlation functions such as $\Gamma_i^{\varepsilon}(t) = \langle S_0^{\varepsilon}(t) S_i^{\varepsilon}(0)\rangle / \langle (S_0^{\varepsilon})^2 \rangle$, or their frequency Fourier transforms $\Phi_i^{\varepsilon}(\omega)$. The more spectacular point is that the $\Phi_i^{\varepsilon}(\omega)$ functions, which are the spectral densities of the spin motion, are expected to diverge as $\omega \to 0$, in one- and two-dimensional systems. This divergence comes from the very slow decay of the correlation functions as $t \to \infty$. A diffusion process which is expected to correctly describe the long-time low-frequency behavior of the spin motion gives a decrease as $t^{-d/2}$, where d is the dimensionality. The divergence of the spectral densities at zero frequency can be immediately seen by considering the area below the curves which represent the correlation functions. The area is infinite for $d \leq 2$.

More complete treatments have been derived by other authors. Carboni and Richards gave exact numerical calculations for finite chains (up to 11 spins $s = \frac{1}{2}$) and showed that the results may be extrapolated to $N \to \infty$.[1] Tahir-Kheli and McFadden constructed an alternative theory, based upon a two-parameter Gaussian representation of the generalized "diffusivity".[2] Recently, a very complete theoretical derivation has been presented by McLean and Blume.[3] These treatments yield comparable results: basically, that as $\omega \to 0$, $\Phi_i^{\varepsilon}(\omega)$ diverges.

To date, the main experimental verifications of the theory have been based upon an analysis of the EPR line. First, in a study by Rogers, Carboni, and Richards,[4] the frequency dependence of the exchange-narrowed dipolar linewidth of the copper salt $Cu(NH_3)_4SO_4H_2O$ (CTS) could not be explained in terms of the Kubo and Tomita theory with Gaussian correlation functions. This afforded the first evidence of the peculiar behavior of the spin correlation functions in one-dimensional systems. Then a "better" chain was found with the salt $(CH_3)_4NMnCl_3$ (TMMC), in which the one-dimensional character is so pronounced that it has an effect on the EPR line shape. Deviation from Lorentzian line shape was observed, showing that the transverse-magnetization correlation function behaves as $e^{-t^{3/2}}$.[5] An interpretation was proposed that used correlation functions which took into account the chain character of the system.[5] Recently, several other one-dimensional spin systems have been studied in the same way.[6,7]

Although EPR has been revealed to be a useful tool to study dynamic properties, the relationship between the individual spin motion and the EPR line is not direct. It involves four-spin correlation functions. Moreover, the frequency linewidth dependence is originated in the "$\frac{10}{3}$ effect."[8] More direct information would be provided by neutron scattering measurements since the differential

scattering cross section is expressed in terms of two-spin correlation functions.

The idea of the present work is to use the nuclear spins surrounding a given electronic spin as probes which "feel" the fluctuating electronic magnetic field. The resulting nuclear relaxation rate, under certain conditions which will be detailed in Sec. II can be expressed as

$$(T_1)^{-1} = A\Phi_0^x(\omega_N) + B\Phi_0^+(\omega_e) , \tag{2}$$

where the $\Phi_0^\alpha(\omega)$ are the frequency self-correlation functions of the spin components s_0^α, with $\alpha = z, +$, and ω_e and ω_N are the electronic and nuclear Larmor frequencies in the static magnetic field H_0; A and B are terms of coupling between the nuclear and the electronic spins. Spin-dynamics studies through longitudinal and transverse nuclear relaxation-time measurements have already been published. For instance Myers and Narath[9] achieved the exchange spectrum in paramagnetic GdP by measuring the ^{31}P nuclei relaxation times as a function of the magnetic field. The ^{19}F linewidth in MnF_3, $KMnF_2$, and $RbMnF_3$ was measured by Hone and Silbernagel as a function of the temperature in order to study the temperature dependence of the microscopic correlation functions.[10] These works, however, were concerned with three-dimensional-lattice spin systems.

In the case of one-dimensional spin systems interest must be concentrated on the low-frequency part of the exchange spectrum, that is, at ω_N. This leads us to consider nuclei with predominant dipolar hyperfine coupling [since the term A in (2) only comes from dipolar coupling]. Consequently, the T_1 value will depend on the exchange spectrum at both frequencies ω_e and ω_N. Since ω_N ($\sim 10^7$ rad/sec) is a very low frequency compared to the linear exchange frequency $\omega_x = J_0/\hbar \gtrsim 10^{11}$ rad/sec the theoretically predicted divergence of $\Phi_0^\alpha(\omega)$ as $\omega_x \to 0$ should result in an extremely short relaxation time, getting shorter and shorter as ω_N is decreased. Experimentally, in "real" chains of spins, finite relaxation times are observed which do not go towards zero as $\omega_N \to 0$. This indicates that in the systems under investigation the divergence breaks down at a frequency larger than ω_N. Therefore, $\Phi_0^x(\omega_N) \simeq \Phi_0^x(0)$. In order to determine both $\Phi_0^x(0)$ and $\Phi_0^+(\omega_e)$ we need two independent experimental measurements. The first is provided by the nuclear relaxation time (T_1), and the second is supplied by the NMR enhancement obtained by dynamic nuclear polarization (DNP). The relationship between these two quantities and the spectral densities will be derived in Sec. II. It is important to note that the couplings between the electronic and nuclear spins are supposed to be known. This means that a determination of the hyperfine coupling tensors have been previously performed. This is discussed in Sec. III, in which the solid free radical Tanol and its magnetic properties are reviewed. The experimental results obtained from the DNP experiments and T_1 measurements are related in Sec. V. In particular, the divergence of $\Phi_0^x(\omega)$ as $\omega \to 0$ is not actually observed. The finite value of $\Phi_0^x(0)$ is interpreted by introducing a "cutoff" process in the spin-motion correlation. In Appendix B we present a derivation of the cutoff effect, and different possible causes of the breakdown in the linear diffusion process are examined. The influence of interchain interactions of the EPR line shape was discussed recently by Hennessy, McElwee, and Richards.[6] We used the same kind of physical considerations, but through alternative experimental methods.

II. NUCLEAR RELAXATION AND OVERHAUSER EFFECT DUE TO EXCHANGE

The reservoir-network model is a convenient way of deriving the general expressions of the nuclear relaxation rate and of the Overhauser enhancement.[11,12] We consider a solid containing N_s electronic spins $\vec{s}_i$ and N_I nuclear spins $\vec{i}_\mu$ in a static magnetic field H_0. The electronic spins are in mutual interactions: exchange E and dipolar D interactions. We assume $E \gg D$. The modulation of the spin component s_i^α ($\alpha = z, +$) comes essentially from the adiabatic part of these interactions: $F = E + D^0$, where D^0 is the secular part of the dipolar term,

$$s_i^\alpha(t) = e^{iFt/\hbar} s_i^\alpha e^{-iFt/\hbar} . \tag{3}$$

We may define three reservoirs corresponding to the electronic and nuclear Zeeman interactions (Z_e and Z_N), and to the spin-spin interactions. These reservoirs are coupled by the electronic nuclear couplings:

$$\mathcal{H}_{eN} = \sum_{i\mu} \vec{s}_i \underline{K}_{i\mu} \vec{i}_\mu , \tag{4}$$

where $\underline{K}_{i\mu}$ denotes the tensor of coupling between $\vec{s}_i$ and $\vec{i}_\mu$. It is suitable to decompose $\mathcal{H}_{eN}$ into terms having characteristic commutation rules with the three reservoirs Z_e, Z_N, and F:

$$\mathcal{H}_{eN} = K_0 + K_1 + K_2 + K_3 , \tag{5}$$

where

$$K_0 = \sum_{i\mu} k_0^{i\mu} s_i^x i_\mu^x ,$$

$$K_1 = \sum_{i\mu} k_1^{i\mu} s_i^x i_\mu^z + \text{c. c.} ,$$

$$K_2 = \sum_{i\mu} k_2^{i\mu} s_i^z i_\mu^z + \text{c. c.} ,$$

$$K_3 = K_{3+} + K_{3-}$$

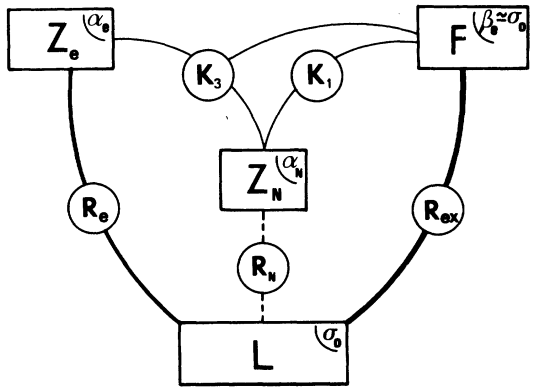

FIG. 1. Reservoir network describing the dynamical nuclear polarization (Overhauser effect) and the nuclear relaxation due to the electronic spins. Z_e is the electronic Zeeman reservoir, Z_N the nuclear Zeeman reservoir. F contains the exchange interactions and the secular part of the dipolar couplings: $F = E + D^0$. L is the lattice. K_1 and K_3 are parts of the hyperfine couplings [see Eq. (5)].

with

$$K_{3\pm} = \sum_{i\mu} k^{i\mu}_{3\pm} s^+_i I^{\pm}_{\mu} + \text{c. c.}$$

The K_1 term which is purely dipolar commutes with Z_e, but not with Z_N or F. So, it introduces a binary coupling between these two reservoirs. The K_3 term does not commute with any of the three reservoirs: It introduces a ternary coupling. The two remaining terms K_0 and K_2, which commute with Z_N, do not connect this reservoir; therefore one may neglect their influence. These commutation rules enable us to set up the network of couplings which is represented in Fig. 1. The lattice reservoir L and its couplings with the spin reservoirs have been represented. The exchange-lattice coupling will be assumed to be efficient enough to maintain the exchange reservoir at the same temperature as the lattice. This assumption may not be valid at low temperature, [13] but in the present study we restrict ourselves to high-temperature regions ($T > 200$ K).

Let us denote by α_e and α_N the inverse temperatures of Z_e and Z_N, and by σ_0 the inverse temperature common to the lattice and to F. In the high-temperature approximation and neglecting the direct nuclear relaxation towards the lattice, the evolution of α_N is given by[11,12]

$$\frac{d\alpha_N}{dt} = -(\alpha_N - \alpha_e)(W^{K_{3+}}_{Z_N Z_e} + W^{K_{3-}}_{Z_N Z_e}) - (\alpha_N - \sigma_0)(W^{K_{3+}}_{Z_N F} + W^{K_{3-}}_{Z_N F} + W^{K_1}_{Z_N F}) , \quad (6)$$

where $W^{K_q}_{PQ}$ are constants of evolution from P to Q reservoirs ($P, Q = Z_N, Z_e, F$) through the coupling K_q ($q = 3+, 3-, 1$). They are expressed in terms of the products of coupling constants ("geometrical factors") with spectral densities

$$W^{K_{3\pm}}_{Z_N Z_e} = \mp 2\pi \frac{\omega_e}{\omega_N} \sum_i \Omega^i_{3\pm} \Phi^+_i(\omega_e \pm \omega_N) ,$$
$$W^{K_{3\pm}}_{Z_N F} = \pm 2\pi \frac{\omega_e \pm \omega_N}{\omega_N} \sum_i \Omega^i_{3\pm} \Phi^+_i(\omega_e \pm \omega_N) , \quad (7)$$
$$W^{K_1}_{Z_N Z_e} = 2\pi \sum_i \Omega^i_1 \Phi^x_i(\omega_N) ,$$
$$W^{K_{3+}}_{PQ} + W^{K_{3-}}_{PQ} = W^{K_3}_{PQ}$$

with

$$\Phi^{\alpha}_i(\omega) = \frac{1}{2\pi} \int_{-\infty}^{+\infty} \Gamma^{\alpha}_i(t) e^{i\omega t} dt , \quad (8)$$

$$\Gamma^{\alpha}_i(t) = \frac{\langle s^{\alpha}_0(t) s^{\alpha *}_i(0) \rangle}{\langle s^{\alpha}_0 s^{\alpha *}_0 \rangle} \quad (9)$$

and

$$\Omega^i_q = \tfrac{4}{3} s(s+1) \frac{N_s}{N_I} \sum_{\mu} \frac{(k^{0\mu}_q)(k^{i\mu}_q)^*}{\hbar^2} + \text{c. c.} ,$$
$$\Omega^0_q = \tfrac{4}{3} s(s+1) \frac{N_s}{N_I} \sum_{\mu} \frac{|k^{0\mu}_q|^2}{\hbar^2} \quad \text{for } i = 0 . \quad (10)$$

A. Nuclear relaxation time

At thermal equilibrium all the temperatures are the same: $\alpha_N = \alpha_e = \sigma_0$. The nuclear relaxation time is the recovery time of α_N after an initial disturbance which makes $\alpha_N \neq \sigma_0$ at $t = 0$:

$$\frac{d\alpha_N}{dt} = -\frac{\alpha_N(t) - \sigma_0}{T_1} . \quad (11)$$

Setting $\alpha_e = \sigma_0$ in (6) and comparing it to (11), one has

$$(T_1)^{-1} = W^{K_3}_{Z_N Z_e} + W^{K_3}_{Z_N F} + W^{K_1}_{Z_N F} . \quad (12)$$

Using (7) one obtains the general expression

$$(2\pi T_1)^{-1} = \sum_i (\Omega^i_{3+} + \Omega^i_{3-}) \Phi^+_i(\omega_e) + \frac{1}{2} \sum_i \Omega^i_1 \Phi^x_i(\omega_N) , \quad (13)$$

where we have made the approximation $\Phi_i(\omega_e \pm \omega_N) \simeq \Phi_i(\omega_e)$.

B. Overhauser-effect enhancement

When the EPR line is saturated by microwave pumping, a new thermal equilibrium is obtained and the NMR signal intensity, which is proportional to α_N, is modified. We define the Overhauser-effect enhancement ρ as $\rho = (\alpha_N - \sigma_0)/\sigma_0$. Its expression is drawn from (6) while at a steady-state regime ($d\alpha_N/dt = 0$) and from (7) and by assuming complete saturation of the EPR line ($\alpha_e = 0$):

$$\rho = \frac{\omega_e}{\omega_N} \frac{\sum_i (\Omega^i_{3+} - \Omega^i_{3-}) \Phi^+_i(\omega_e)}{\sum_i (\Omega^i_{3+} + \Omega^i_{3-}) \Phi^+_i(\omega_e) + \frac{1}{2} \sum_i \Omega^i_1 \Phi^x_i(\omega_N)} . \quad (14)$$

Experimentally the enhancement at complete saturation can be obtained by measuring the enhancement as a function of the microwave power

and extrapolating it for infinite pumping power.

In the case of strong isotropic exchange interaction $\Phi_i^+(\omega) \simeq \Phi_i^z(\omega)$ and thus the labels + or z may be dropped. The general expressions (13) and (14) imply not only the frequency self-correlation function $\Phi_0(\omega)$, but also all the cross functions $\Phi_i(\omega)$. In the following, we will assume that the influence of the cross terms may be neglected. This simplifying assumption may be justified by the decrease of the geometrical factors $\Omega_q^i (\sim i^{-3})$. As for the spectral densities $\Phi_i(\omega)$, their values at low frequency ($\omega \simeq 0$) do not decrease appreciably with increasing i. In addition, it must be noted that (13) and (14) suppose that a single nuclear reservoir is involved, or, in other words, that all the nuclear spins are at the same temperature. This implies an efficient cross-relaxation mechanism among the nuclear spins. The nuclear-nuclear coupling must be always stronger than the nuclear-electronic coupling. If not, it should be necessary to define several Zeeman nuclear reservoirs, say, n. Every nuclear reservoir $Z_N^{(i)}$ ($i = 1, 2, \ldots, n$) has its own temperature $\alpha_N^{(i)}$. At thermal equilibrium all the $\alpha_N^{(i)}$ are the same: $\alpha_N^{(i)} = \sigma_0$. But under dynamic polarization one may have $\alpha_N^{(i)} \neq \alpha_N^{(j)}$. Such a situation gives rise to "distorted" NMR lines. As it will be related in Sec. IV, this case was observed in Tanol for some orientations of the crystal axis with respect to the static magnetic field. A complete treatment of the effect is feasible,[14] taking into account all the possible nuclear reservoirs and their mutual couplings (nuclear cross-relaxation terms). The n different nuclear-spin temperatures are obtained by solving the system of the n equations of evolution. Nevertheless the present discussion is limited to the case where a single nuclear-spin temperature is sufficient to describe the system under polarization. Experimentally this simplified situation is rather well approached in Tanol when the crystal-axis orientation corresponds to the maximum (negative) enhancement of the NMR lines.

Thus, under the conditions of (i) strong isotropic (Heisenberg) spin-exchange Hamiltonian, (ii) negligible cross terms, and (iii) strong nuclear cross relaxation, we obtain the simplified expressions

$$(2\pi T_1)^{-1} = (\Omega_{3+} + \Omega_{3-})\Phi_0(\omega_e) + \tfrac{1}{2}\Omega_1\Phi_0(\omega_N)\,, \qquad (15)$$

$$\rho = \frac{\omega_e}{\omega_N} \frac{(\Omega_{3+} - \Omega_{3-})\Phi_0(\omega_e)}{(\Omega_{3+} + \Omega_{3-})\Phi_0(\omega_e) + \tfrac{1}{2}\Omega_1\Phi_0(\omega_N)}\,, \qquad (16)$$

where all the terms are autoterms. It clearly appears from (15) and (16) that, if the geometrical factors Ω_q are known, by measuring T_1 and ρ, the values of the frequency self-correlation function can be determined at the two frequencies ω_e and ω_N.

III. PROPERTIES OF TANOL

The sample chosen for this kind of study must fulfill the following conditions: (i) Magnetic properties correspond to a one-dimensional Heisenberg Hamiltonian, (ii) hyperfine coupling is known and has a mainly dipolar character, and (iii) electronic relaxation times (T_{1e} and T_{2e}) are not too short so that saturation of the EPR line can be achieved with reasonable microwave power. The third point leads us to organic free radicals since in such compounds the spin-orbit coupling is weak enough not to contribute to the spin-lattice relaxation time. The required dipolar character of hyperfine couplings excludes the free radicals of aromatic types. In all these respects the nitroxyde free radical 2, 2, 6, -tetramethyl-4-piperidinol-1-oxyl (Tanol) is a good sample. Furthermore, Tanol has the advantage that in a single crystal all the molecules are parallel to each other. The unpaired electronic spin $s = \frac{1}{2}$ is located on the nitroxyde bond. As represented in Fig. 2, there are 18 protons per molecule, the NMR signal of which will be observed in our experiments. The lattice is monoclinic with parameters $a = 7.10$ Å, $b = 14.0$ Å, $c = 5.84$ Å, and $\beta = (\vec{a}, \vec{c}) = 119.8°$. There are two molecules per unit cell located at (0, 0, 0) and (a, $\frac{1}{2}b$, 0). The $(\vec{a}, \vec{c})$ plane is a mirror plane for both the crystal lattice and the molecule.[15] The positions of the protons have been determined.[16] Two protons are located in the mirror plane: $H(O_1)$ and H(1). The 16 others can be arranged in eight pairs symmetrically with respect to the mirror plane. A projection to the mirror plane $(\vec{a}, \vec{c})$ is represented in Fig. 3.

The coupling between the electronic spins and the protons requires 18 tensors of coupling, but only ten are different because of the symmetry. We determined these couplings by recording the NMR spectra of single crystals of Tanol at helium temperature as a function of the static magnetic field direction in three crystallographic planes.[17] Given any direction (θ, ϕ) the line of a proton μ is shifted by an amount

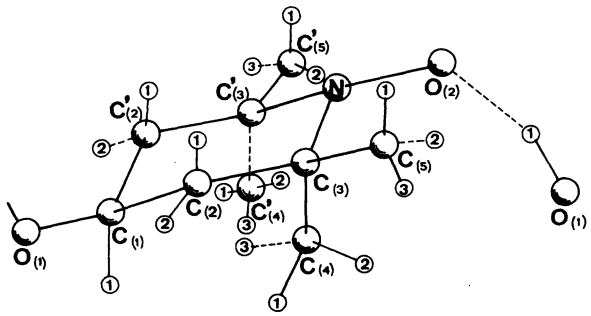

FIG. 2. Tanol molecule (2, 2, 6, 6-tetramethyl-4-piperidinol-1-oxyl).

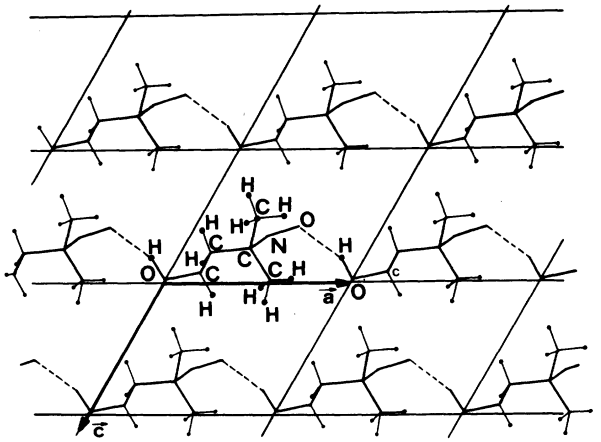

FIG. 3. Structure of Tanol crystal viewed along $\vec{b}$ axis. [Projection on the mirror plane $(\vec{a}, \vec{c})$.]

$$\Delta H^{\mu}(\theta, \phi) = (\hbar \gamma_N)^{-1} \langle s^{z} \rangle \sum_i k_0^{i\mu}(\theta, \phi) , \qquad (17)$$

where γ_N is the nuclear gyromagnetic ratio and where $\langle s^{z} \rangle \sim \chi H_0$, with χ the magnetic susceptibility. From the angular variation of ΔH^{μ}, it is theoretically possible to determine the tensor which describes the coupling of a proton with the ensemble of the electronic spins $\underline{K}_{\mu} = \sum_{\lambda} \underline{K}_{\lambda\mu}$; that is to say, to determine its three principal values and the three angles which define the direction of its principal axes. But this would mean that the angular variation of the NMR-line positions of every proton would have to be followed without any ambiguity. As the NMR spectra were only partially resolved (we operated in 16.6-kG magnetic field), the problem could not be solved entirely for every proton. Therefore, we resorted to a simplified model. We assumed it was possible to account for the traceless part of $\underline{K}_{\mu}$ by calculating the dipolar interactions with electronic spin densities localized on a few points. The best agreement of the calculations with the observed angular variation was obtained with a simple four-point dipolar model by assuming (i) spin density $\simeq 0.3$ and 0.7 on the nitrogen and on the oxygen atoms, respectively, and (ii) electronic spin located in the π orbital lobes at points separated by 1.2 Å. We have considered the electronic spin located on the same molecule as a given proton and the electronic spins located on the ten neighbors. The calculated angular variation of the shift enabled us to identify most of the protons on the NMR spectra. After a proton has been identified, its measured shifts along any three perpendicular axes give the scalar coupling directly. The obtained values are listed in Table I, column a. Large uncertainties are mentioned for protons H(2-2) and H(4-1) which have not been identified, and for H(4-2) and H(5-1) which have been identified in only one plane. In column b we have listed the values that we used in later calculations. The demagnetizing field (0.5G) has been subtracted by assuming the samples to be spherical, though they are not. The value given for H(4-1) was obtained by subtracting the sum of the values of H(4-2) and H(4-3) from three times the coupling of the C_4 methyl group observed in solution: -0.73 G.[18] For H(2-2) we took the value corresponding to the middle of the uncertainty.

In short, we used a model of the coupling between electronic spins and protons consisting of (i) a scalar part, the values of which are listed in Table I, column b, and (ii) a dipolar part calculated from a four-point model.

Heat-capacity measurements were first performed by Lemaire *et al.*[19] as low as 1.3 K. For the heat capacity of magnetic origin, they obtained a curve $C_M = f(T)$ which showed a broad maximum near 4 K, and which was explained in terms of an antiferromagnetic exchange interaction between neighboring spins along linear chains. The agreement with the theoretical calculations of Bonner and Fischer[20] gave $J/k = 4.16$ K. This behavior was confirmed by magnetic susceptibility measurements.[21] Recently, heat capacity measurements have been extended as low as 0.35 K.[22] A sharp peak appears at 0.49 K, which gives the Néel temperature.

IV. EXPERIMENTAL

The DNP experiments, which will be reported here, were performed in a magnetic field of about 1 kG. The electronic pumping frequency was supplied by a carcinotron and amplified to 10W–15W in a traveling-wave tube. It generated a rotating magnetic field of about 5 G in a reentrant cavity. The device was a wide-line DNP spectrometer which enabled us to perform measurements in the

TABLE I. Scalar coupling constants of the protons of Tanol in the solid state (Ref. 17). Berliner's notations are used (Ref. 16).

	a (Oe)	b (Oe)
H(01)	-1.48 ± 0.1	-2.0
H(1)	0.82 ± 0.1	$+0.3$
H(2-1)	0.0 ± 0.3	-0.5
H(2-2)	$-1.5 \cdots 0.0$	-1.3
H(4-1)	$-1.5 \cdots 0.0$	-0.8
H(4-2)	0.2	-0.3
H(4-3)	-0.5 ± 0.3	-1.0
H(5-1)	0.6	0.0
H(5-2)	-0.5 ± 0.3	-1.0
H(5-3)	2.45 ± 0.2	$+2.0$

[a]Experimental results.

[b]Values actually used in the computation after taking into account demagnetizing field effect.

frequency range between 2 and 8 GHz.[23] NMR signal was detected with a frequency-scanned Robinson oscillator and recorded after lock-in detection. In typical record the signal-to-noise ratio of the unpolarized signal P_0 was ~10. The Overhauser-effect enhancement (ρ) corresponding to an infinite pumping power was obtained by extrapolating the curve $[P(W)/P_0 - 1]^{-1}$ as a function of W^{-1}, where $P(W)$ is the polarized signal intensity with a pumping power W. In case of distortion of the polarized signal double integration was performed from the lock-in derivative signal. At maximum pumping power the saturation factor was no larger than 0.3. This leads to an uncertainty of about ±20% on the extrapolated enhancement value. We performed DNP experiments on a powder sample and on single crystals. Several crystals were used. They had been selected because of a particular morphology. Two favorable cases may occur: either long crystals which were grown with the $\vec{c}$ axis along the long direction (typical size: 10×3×2 mm), and flat crystals offering the $(\vec{a}, \vec{c})$ plane as cleaving plane (typical size: 4×4×2.5 mm). The crystal was affixed to a rod which allowed rotation around the $\vec{c}$ axis (or $\vec{b}$ axis, depending on the type of the crystal) inside the rf coil. A strong flow of cold nitrogen gas was blown on the sample to avoid heating by microwave power. The temperature was controlled by a thermocouple which was inserted inside the sample, and regulated in the range 250–300 K.

Nuclear relaxation times were measured with pulse sequences π, $\frac{1}{2}\pi$ in a conventional pulsed NMR spectrometer. Measurements were performed between 4 and 54 MHz.

V. RESULTS AND DISCUSSION

The principle of our method[24] of determining the exchange spectral densities is based upon expressions (15) and (16), from which

$$\Phi_0(\omega_e) = -\tfrac{1}{660}(\Omega_{3+} - \Omega_{3-})^{-1}\rho/2\pi T_1 , \qquad (18)$$

where the factor −660 takes the place of ω_e/ω_N since we are dealing with protons, the "geometrical factors" Ω_{3+} and Ω_{3-} are calculable from the coupling-constant model explained in Sec. III, and the values of ρ and T_1 are given by measurements. The absolute value of $\Phi_0(\omega_e)$ can be deduced. Then $\Phi_0(\omega_N)$, which is $\simeq \Phi_0(0)$, is obtained from (15).

It turned out that the nuclear-signal enhancement is strongly dependent on the orientation of the crystal with respect to the static magnetic field, and that it is negative for most of the orientations.[24,25] These two experimental facts are consistent with the mainly dipolar character of the electronic-nuclear couplings. The polarized NMR signal has been recorded for different orientations when the crystal is rotated around its $\vec{b}$ axis. The maximum enhancement occurs when the $\vec{c}$ axis is about parallel to H_0. Its extrapolated value is

$$\rho_{max} = -100 \pm 20 .$$

At orientations corresponding to small enhancements (the region perpendicular to the $\vec{c}$ axis) we observed distorted polarized NMR signals. Some of them may be clearly interpreted as the superposition of negative and positive signals, showing thus the coexistence of several nuclear-spin temperatures in the sample. The quantitative interpretation of this effect requires calculations which take into account several nuclear reservoirs and their cross relaxation, as well electronic cross-correlation terms.[14] As the purpose of the present paper is not a study of the Overhauser effect in itself but its use as a tool for getting information about spectral densities we will restrict ourselves to the region of the $\vec{c}$-axis approximately parallel to H_0, where apparently, only one nuclear-spin temperature is sufficient to describe the system. Therefore expressions (15), (16), and (18) are valid. So, all the quantities involved in (18) should be considered at that particular direction. But, because of a poor signal-to-noise ratio, it was not possible to measure the nuclear relaxation time on single crystals at the frequency corresponding to the DNP experiments, 4.1 MHz. Nevertheless the anisotropy of T_1, measured at higher frequencies, turned out to be small, of the order of 10%. Therefore we will take the value of T_1 measured at 4.1 MHz on a powder sample, $(3 \pm 0.3)\times 10^{-4}$ sec. Then, taking the value of the "geometrical factor" $(\Omega_{3+} - \Omega_{3-})$ calculated in the direction under consideration, we found $\Phi_0(\omega_e) = (1 \pm 0.4)\times 10^{-12}$ (rad/sec)$^{-1}$, which in reduced units $\omega_e^* = \omega_e/\omega_x$ with $\omega_x = J/\hbar$ $= 5.2\times 10^{11}$ rad/sec, yields[12]

$$\omega_x \Phi_0(0.03) = 0.5 \pm 0.2 . \qquad (19)$$

This value should be compared to theoretical predictions. We calculated $\Phi_0(\omega)$ by taking the Fourier transform of the self-correlation function, which was constructed in the following manner:

$$\Gamma_0(\xi, t) = \tilde{\Gamma}_0(t)\gamma_\xi(t), \qquad (20)$$

where $\tilde{\Gamma}_0(t)$ is the correlation function for an "ideal" Heisenberg chain and $\gamma_\xi(t)$ is a cutoff function which accounts for the breakdown of the spin correlation function. The function $\tilde{\Gamma}_0(t)$ is defined by

$$\tilde{\Gamma}_0(t) = \frac{\langle \tilde{s}_0^{\alpha}(t)\, \tilde{s}_0^{\alpha *}(0)\rangle}{\langle |s^{\alpha}(0)|^2\rangle} , \qquad (21)$$

where the time development is governed only by the linear Heisenberg Hamiltonian (1). Thus

$$\tilde{s}_0^{\alpha}(t) = e^{iE_c t/\hbar} s_0^{\alpha} e^{-iE_c t/\hbar} .$$

For $\tilde{\Gamma}_0(t)$ we took the time self-correlation function

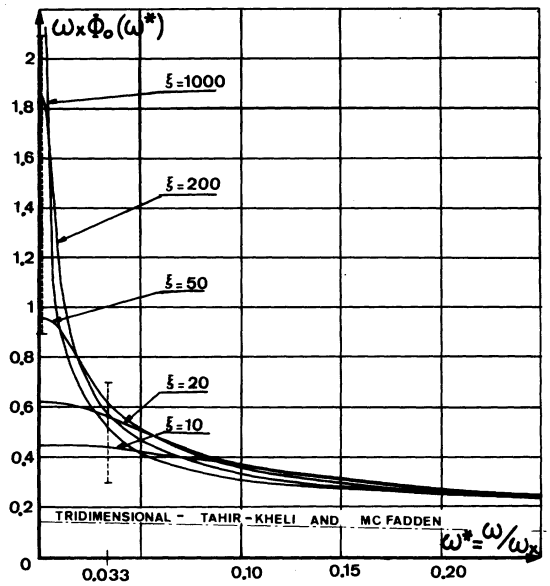

FIG. 4. Fourier transform of the self-correlation function $\Gamma_0(\xi, t)$ [Eq. (20)] for different values of the cut-off parameter $\xi = \omega_x/\omega_c$. Dashed lines correspond to the experimental results (19).

calculated from the results of Tahir-Kheli and McFadden (Fig. 8 of Ref. 2). For long times, $(J_0/\hbar)t > 3$, we extended the curve by a $t^{-1/2}$ law expressing a linear diffusive behavior. The diffusion coefficient evaluated in this way is close to the value expected, for spin $s = \frac{1}{2}$, from the method of McFadden and Tahir-Kheli,[2]

$$D \simeq \sqrt{\pi}\,(J_0/\hbar)c^2 \simeq 1.77(J_0/\hbar)c^2\,, \tag{22}$$

where c is the space between two neighboring spins in a chain.

The cutoff function $\gamma_\xi(t)$ describes the decay rate at which the spin motion is deviated from its one-dimensional diffusive behavior. We define a characteristic "cutoff frequency" ω_c and a cutoff dimensionless parameter $\xi = \omega_x/\omega_c$. For the moment ξ is just a phenomenological parameter which can be determined experimentally. We first took for the cutoff an arbitrary experimental shape[12,26]

$$\gamma_\xi(t) = e^{-t\omega_x/\xi}\,.$$

In fact, as shown in Appendix B, an expression such as

$$\gamma_\xi(t) = e^{-(t\omega_x/\xi)^{3/2}}$$

may be more appropriate to describe the cutoff process in nearly-one-dimensional systems. But, whatever the actual expression used for $\gamma_\xi(t)$, the behavior of $\Gamma_\xi(\xi, t)$ is hardly changed.

Thus, by Fourier transform of (20), one obtains the frequency self-correlation functions $\Phi_0(\xi, \omega)$, which have been represented in Fig. 4 for small values of the reduced frequency $\omega^* = \omega/\omega_x$, and for different ξ. One notes that, for $\omega^* \gtrsim 0.05$, $\omega_x\Phi_\xi(\omega^*)$ depends very little on ξ. But it is not the same thing for $\omega \to 0$: $\Phi_0(\xi, 0) \sim \xi^{1/2}$. Note that our experimental result (19) is in good agreement with the one-dimensional character of the spin system, but it cannot afford information on ξ, that is, on the "perfectness" of the chain. The value of ξ must be drawn from the zero-frequency limit of $\omega_x\Phi_0(\xi, \omega^*)$. The latter could be obtained by putting the result (19) in Eq. (15), where $\Phi(\omega_N) \simeq \Phi(0)$. But a more accurate determination is obtained by considering the frequency dependence of T_1.

The experimental nuclear relaxation rate $(T_1)^{-1}$ has been plotted in Fig. 5 as a function of $\omega_e^* = \omega_e/\omega_x$, where $\omega_e = 660\omega_N$. The solid lines have been calculated from

$$\langle 1/2\pi T_1 \rangle_\xi = \langle \Omega_{3+} + \Omega_{3-} \rangle \Phi_0(\xi, \omega_e^*) + \tfrac{1}{2}\langle \Omega_1 \rangle \Phi_0(\xi, 0)\,, \tag{23}$$

where the symbols $\langle\ \rangle$ refer to powder averages of the geometrical factors. By taking into account the couplings of the protons with the electronic spin of their own molecule and with those belonging to the ten neighboring molecules, we found

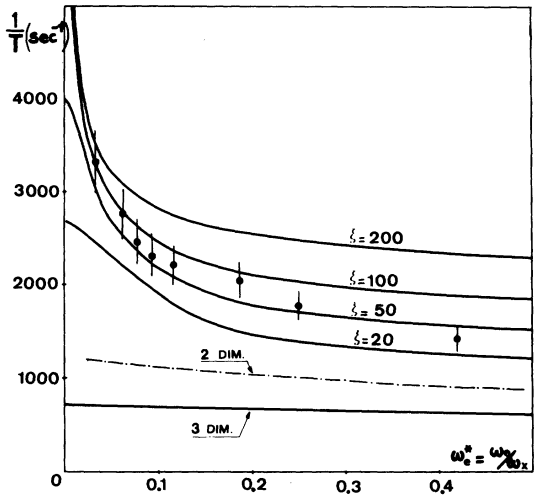

FIG. 5. Proton spin-lattice relaxation rate of Tanol powder sample as a function of the reduced electronic Larmor frequency: $\omega_e^* = \omega_e/\omega_x$, with $\omega_e = \gamma_e H_0$ and $\omega_x = J/\hbar = 5.2 \times 10^{11}$ rad/sec ($\omega_e^* = 0.1$ corresponds to $H_0 = 2.94$ kG.) The theoretical curves have been calculated from expression (23) using the powder average of the geometrical factors (hyperfine coupling) of Tanol. The dashed curve (two-dimensional) has been obtained by assigning a reasonable, but arbitrary, cutoff to the frequency correlation functions of a two-dimensional system given by Tahir-Kheli and McFadden (Ref. 2). [If no cutoff is assumed $\Phi_0(0)$ is infinite in two dimensions.] Thus, strictly speaking, only the frequency dependence of the dashed curve is significant to exclude two-dimensional exchange in Tanol.

$\gamma_e^{-2}\langle\Omega_{3+}+\Omega_{3-}\rangle = 1.0\ \mathrm{G}^2$ and $\gamma_e^{-2}\langle\Omega_1\rangle = 0.6\ \mathrm{G}^2$. The values of $\Phi_0(\xi, \omega_e^*)$ and $\Phi_0(\xi, 0)$ are the same as in Fig. 4. From the experimental points (Fig. 5) we may deduce that $\xi \simeq 50$, and therefore

$$\hbar\omega_c/k = (J_0/k)/\xi \simeq 0.08\ \mathrm{K}\ . \tag{24}$$

To interpret this result we have to analyze the physical reasons why the linear diffusion process breaks down. In the following we review cutoff processes which arise when one deals with *real* samples. (i) The chains are not perfectly isolated, and one has to account for small *interchain* couplings. (ii) The diffusion behavior may be disturbed inside the chain itself because the Hamiltonian is not purely isotropic. Deviations from the ideal Heisenberg Hamiltonian (1) result from both anisotropic terms (Ising-like) in the exchange Hamiltonian and *intrachain* dipolar couplings. Finally, (iii) the chains of spins are not infinite, and some *finite* length effects may be expected.

(i) The interchain interactions, by changing the linear diffusion process into a three-dimensional process, lead to cutoff effects. Such phenomena were first discussed by Hennessy, McElwee, and Richards in a study of the line shape of the electronic paramagnetic resonance in nearly-one-dimensional systems.[6] In Appendix A we adopt the calculation of these authors to the two-spin correlation functions. In Appendix B, we present a different calculation of the cutoff effects, performing the derivation directly on the correlation functions $\Gamma_i^{\alpha}(t)$. In both derivations similar cutoff functions are obtained:

$$\gamma_t(t) = e^{-(\omega_c t)^{3/2}}\ , \tag{25}$$

where $\omega_c = \omega_x/\xi$ is the cutoff frequency. However, our derivation gives a larger value for ω_c. For interchain Heisenberg couplings between nearest neighbors, where J_1 and J_2 are the exchange integrals along two directions perpendicular to the chain axis, we get for $s = \frac{1}{2}$ and with D given by (22) [Appendix B, Eq. (B12)]

$$\omega_c \simeq 4.7(1+\alpha^2)^{2/3}(J_1/\hbar)(J_1/J_0)^{1/3}\ , \tag{26}$$

where $\alpha = J_1/J_2$. If we assume that $J_1 = J_2 = J'$ ($\alpha = 1$), the interchain coupling may be evaluated, in Tanol, by

$$J'/k \simeq 3.6\times10^{-2}\ \mathrm{K}. \tag{27}$$

In order to obtain some information on the ratio $\alpha = J_2/J_1$, we will use another independent evaluation of the interchain interactions based upon the values of the Néel temperature ($T_N = 0.49$ K [22]) and of the intrachain exchange ($J_0/k = 4.1$ K [19]). Oguchi[27] first proposed a derivation to calculate the interchain coupling for a Heisenberg interaction between nearest neighbors. In Ref. 6 this calculation is extended to the case of two distinct interchain couplings J_1 and J_2:

$$kT_N/J_0 = \tfrac{4}{3}s(s+1)f/I\ , \tag{28}$$

with $I = 0.64(J/J_1)^{1/2}\,[1+0.253\ln(J_1/J_2)]$, where it is assumed that $J/J_1 \ll 1$ and $\alpha = J_2/J_1 < 1$. In Ref. 6, the function f is discussed as decouplings of Green's functions: $f = 1$ in the random-phase approximation (RPA) and $f = 1 + [(s-1)/3s][(I-1)/I]$ according to a Tahir-Kheli (TK) suggestion.[28]

From the two independent measurements T_1 and T_N, it is possible to specify the interchain couplings J_1 and J_2. The values of J_1 and J_2 which are compatible with both Eq. (26) and Eq. (28) are given in Table II.

TABLE II. Values of the interchain couplings J_1 and J_2 which are consistent with both the cutoff frequency obtained from nuclear-relaxation data $\omega_c \approx \omega_x/50$ [see Eq. (26)], and the Néel temperature $T_N = 0.49$ K. Equation (28) has been used either in the random-phase approximation (RPA) or with a Tahir-Kheli (TK) derivation (Ref. 28).

RPA	TK
$J_1/k = 3.4\times10^{-2}$ K	$J_1/k = 4.5\times10^{-2}$ K
$J_2/k = 1.8\times10^{-2}$ K	$J_2/k = 3.8\times10^{-2}$ K

We see that the two methods (RPA and TK) lead to very similar results. The values of J_1 and J_2, which are about the same within a factor of 2, can be compared to the interchain dipolar couplings. In Tanol, the exchange chains are along the $\vec{c}$ axis.[14] There are two neighboring chains in the mirror plane, corresponding to the $\pm\vec{a}$ translations, and four off-plane neighboring chains. We define J_{1d} and J_{2d} as in-plane and off-plane dipolar couplings, respectively. These can be evaluated by the summation

$$J_{id} = \tfrac{1}{2}g\mu_B\left(\sum_{n=-\infty}^{+\infty}\frac{1}{|\vec{r}_{in}|^6}\right)^{1/2}\quad (i=1,2)\ ,$$

where vector $\vec{r}_{in}$ joins the electronic spin located at the origin to the nth spin of a chain i. We obtained

$$J_{1d}/k = 7.5\times10^{-3}\ \mathrm{K}\ ,$$

$$J_{2d}/k = 3.9\times10^{-3}\ \mathrm{K}\ .$$

Comparing these values with Table II, we may conclude that the interchain dipolar coupling cannot explain both the cutoff effect on the one-dimensional spin diffusion and the value of the Néel temperature.

(ii) Let us now examine the role of intrachain interactions. The total intrachain Hamiltonian will be denoted as $\mathcal{H}_c$. The assumption of a diffusion process requires that, in the chain, the total magnetic flux be conserved. This property

is expressed as follows:

$$\frac{d}{dt}\sum_i \langle e^{i\mathcal{H}_c t/\hbar} s_i^\alpha e^{-i\mathcal{H}_c t/\hbar} s_0^{\alpha *}\rangle = 0 \ . \tag{29}$$

This fundamental condition is satisfied by the commutation rule

$$[S^\alpha, \mathcal{H}_c] = 0 \quad (\alpha = z, +) \ . \tag{30}$$

If $\mathcal{H}_c$ is only a Heisenberg Hamiltonian, such as (1) ($\mathcal{H}_c = E_c$), one has $[S^\alpha, E_c] = 0$. The correlation functions for any component of the spin ($\alpha = z, +$) may be described by a one-dimensional diffusive behavior. On the other hand, if $\mathcal{H}_c$ contains an extra term which does not commute with S^α, the correlation function $\Gamma_i^\alpha(t)$ will deviate from a pure one-dimensional diffusive behavior. Thus, the intrachain dipolar interactions give rise to cutoff effects. The cutoff function, as shown in Appendix B, is still of the form (25). The cutoff frequency is angularly dependent and also depends on the amplitude of the magnetic field H_0. In Appendix B, we give the complete expression of ω_c, which we relate to the expression of the EPR linewidth. Using the result that the EPR linewidth in Tanol is smaller than 3 Oe we obtain an upper bound of the cutoff frequency for the autocorrelation function:

$$\hbar\omega_c/k < 0.026 \text{ K} \ .$$

Hence by comparing this value and the result (24), we conclude that, in Tanol, the intrachain dipolar couplings cannot explain the cutoff effect of the correlation functions.

The cutoff effect cannot be explained either by a small Ising-like extra term $\Delta J_0 \sum s_i^x s_{i+1}^x$, an order of magnitude of which may be deduced from the anisotropy of the g tensor[29]: $\Delta J_0 \sim (\Delta g/g)^2 J_0$, where Δg is the deviation of g from the value for a free electron. The three principal g values are $g_{xx} = 2.006$, $g_{yy} = 2.003$, and $g_{zz} = 2.009$[30]; this leads to $\Delta J_0/k \sim 10^{-4}$–$10^{-5}$ K. This value turns out to be much smaller than the intrachain dipolar interactions $(\hbar\gamma_e)^2/c^3 k = 1.25\times 10^{-2}$ K, which have been shown not to be large enough to explain the observed cutoff. Consequently, the anisotropy of the exchange should play a negligible role.

(iii) Finally, we consider the effect of finite chain length. The effect of limiting the number of spins in the chain is also to introduce a cutoff by preventing the frequency correlation function $\phi_i^\alpha(\omega)$ from completely diverging when $\omega \to 0$. The physical reason of this is that the divergence of $\phi_i^\alpha(\omega)$ for $\omega \to 0$ only results from the contribution of the small wave vectors, $|q| \to 0$. With a finite number of spins in the chain, N, the minimum value of $|q|$ is not zero but $q_0 = \pi/Nc$. As a result of this, $\phi_i^\alpha(\omega)$ has a finite value at zero frequency. Using the simple description of the diffusion[31] which is valid as $q \to 0$ and $\omega \to 0$, we may estimate the number of spins per chain, which gives a value of $\phi_0^x(0)$ consistent with experiment: The wave-vector-dependent frequency autocorrelation function is given by

$$\phi_0^x(q, \omega) = \frac{1}{\pi}\frac{Dq^2}{D^2q^4 + \omega^2} \ . \tag{31}$$

The frequency correlation function is obtained by integrating (31) over the first Brillouin zone. With N spins per chain and setting $\omega = 0$ in (31), one has

$$\phi_0^x(0) = \frac{1}{\pi}\frac{c}{\pi}\int_{\pi/Nc}^{\pi/c} \frac{dq}{Dq^2} \ . \tag{32}$$

Taking the expression (22) for D, this leads to

$$N - 1 = \sqrt{\pi}\,\pi^3 (J_0/\hbar)\Phi_0^x(0) \ . \tag{33}$$

With $\xi \approx 50$, one has $(J_0/\hbar)\Phi_0^x(0) \approx 1$ (see Fig. 4) and thus, from (33), we obtain $N \approx 50$. The method of generalized diffusivity, as used by McElwee,[32] predicts a somewhat smaller value, $N \approx 35$.

We now have to compare this number of spins per chain, $N \approx 35$–50, to what is known about the perfectness of the samples of Tanol. According to microanalysis the deviation from the theoretical composition is less than 0.3%. However, this is not a proof of *magnetic* purity. An estimate of this could be provided by static susceptibility measurements. The Curie constant of pure nitroxide free radicals should be $C_M = 0.377$.[21] In Tanol, a somewhat smaller value has been determined,[21] $C_M = 0.36$; but the uncertainty in this figure, which is $\sim 3\%$, does not allow any quantitative conclusion.[33] An indication that the chains are not perfect is given by the fact that an increase of the susceptibility is observed at low temperature[33] ($T < 2$ K). This low-temperature increase, which seems to be typical of one-dimensional magnetic systems, may be interpreted as resulting from finite chains containing an odd number of spins[20] (on the average there is one odd chain per two chains).

Thus, with the experimental data available at present, we cannot exclude the finite length of the spin chains as being responsible for the cutoff effects observed in Tanol.

VI. CONCLUSION

First, we have presented an attempt of a purely experimental determination of the spin correlation in a nearly-one-dimensional Heisenberg system. The method, which is based on both dynamical nuclear polarization and nuclear spin-lattice relaxation-time measurements, has been applied in the crystalline free radical Tanol. A value of the frequency correlation function at $\omega_e/\omega_x = 0.03$ has been obtained which is in agreement with the the-

oretical prediction in one dimension using the calculations of Tahir-Kheli and McFadden. However, owing to the uncertainty in the hyperfine couplings—especially the scalar parts—and to the difficulty of achieving quantitative DNP measurements, it was not possible to obtain the shape of the spin correlation functions over a given frequency range without resorting to a theoretical model. The time correlation function $\Gamma_i(t)$ of a real nearly-one-dimensional system has been expressed as a product of the time correlation function $\tilde{\Gamma}_i(t)$ of the ideal perfectly-one-dimensional system with a cutoff function: $\Gamma_i(t) = \tilde{\Gamma}_i(t)\, e^{-(\omega_c t)^{3/2}}$. This form has been derived from a perturbation short-time expansion. The cutoff frequency ω_c, which is expressed in terms of the interchain couplings, can be determined experimentally from the fit with nuclear relaxation-time measurements. This procedure constitutes a method for determining interchain couplings at room temperature, that is, at a temperature much higher than the temperature of the three-dimensional magnetic order resulting from the interchain couplings. The interchain couplings are determined through their effect on the high-temperature spin dynamics. Very weak couplings can be detected because they cause a dramatic disturbance on the long-time persistence of the spin correlation due to spin diffusion in one dimension.

Concerning Tanol, first we have shown that the frequency dependence of $(T_1)^{-1}$ at room temperature confirms the one-dimensional character of the exchange Hamiltonian (three- or two-dimensional systems can be clearly excluded; see Fig. 5). Secondly, the magnitude of the cutoff frequency has been determined to be $\omega_c \approx \omega_x/50$. This value, together with the Néel temperature, leads to interchain couplings J_1 and J_2, which are about the same (within a factor 2), and are two orders of magnitude smaller than J. However, the same cutoff effect may correspond to more isolated chains, but the length of which is limited to 35–50 spins.

ACKNOWLEDGMENT

The authors are greatly indebted to M. Plaindoux for the computation of the correlation functions.

APPENDIX A: CALCULUS OF THE CUTOFF FREQUENCY FROM THE HENNESSY, McELWEE AND RICHARDS DERIVATION

The first description of the "cutoff" effect due to small interchain interactions was presented by Hennessy, McElwee, and Richards[6] in a study of the line shape of the electronic paramagnetic resonance in nearly one-dimensional systems. The method of these authors consisted in evaluating the contribution of small interchain interactions E_I on the wave-vector-dependent time correlation function $\langle s^x_{q_x}(t) s^x_{-q_x}(0)\rangle$, where

$$s^x_{q_x}(t) = e^{i(E_c+E_I)t/\hbar}\, s^x_{q_x}\, e^{-i(E_c+E_I)t/\hbar}, \tag{A1}$$

E_c is the linear Heisenberg Hamiltonian, and

$$s^x_{q_x} = \sum_{i=1}^{N_c} s^x_i\, e^{i\vec{q}_x\cdot\vec{r}_i}, \tag{A2}$$

where $\vec{r}_i$ is a vector along the chain. In order to adapt this calculation to the two-spin correlation functions $\Gamma^x_i(t)$ which are defined in Sec. II by Eq. (9), we start from Eq. (33) of Ref. 6:

$$\langle s^x_{q_x}(t) s^x_{-q_x}(0)\rangle = \tfrac{1}{3} s(s+1)\, e^{-Dq_x^2 t}\, \tilde{\Phi}_q(t), \tag{A3}$$

where D is the linear diffusion coefficient. The function $\tilde{\Phi}_q(t)$ is given by Eq. (30) of Ref. 6, where E_I represents Heisenberg Hamiltonian with only nearest-neighbor couplings for an orthorhombic lattice. To calculate the correlation function $\Gamma^x_i(t)$, we use Eqs. (A2) and (A3) as follows:

$$\begin{aligned}\Gamma^x_i(t) &= \langle s^x_0(t) s^x_i(0)\rangle / \langle (s^x_0)^2\rangle \\ &= \frac{abc}{(2\pi)^3}\int_{-\pi/c}^{+\pi/c} dq_x\, e^{-iq_x\cdot r_{0i}}\, e^{-Dq_x^2 t} \\ &\quad\times \int_{-\pi/a}^{+\pi/a} dq_x \int_{-\pi/b}^{+\pi/b} dq_y\, \tilde{\Phi}_q(t),\end{aligned} \tag{A4}$$

where a, b, and c are the lattice parameters of the crystal. Then, the cutoff function $\gamma_i(t)$, which is defined by Eq. (20) of Sec. V, is evaluated as

$$\begin{aligned}\gamma^x_i(t) = \frac{\Gamma^x_i(t)}{\tilde{\Gamma}_i(t)} &= \exp[-(1+\alpha^2)(t/t_0)^{3/2}] \\ &\quad\times I_0\left[\left(\frac{t}{t_0}\right)^{3/2}\right] I_0\left[\alpha^2\left(\frac{t}{t_0}\right)^{3/2}\right],\end{aligned} \tag{A5}$$

where $\tilde{\Gamma}_i(t)$ represents the correlation function for an "ideal" Heisenberg chain [Eq. (21) of Sec. V]. In Eq. (A5) notations are the same as in Ref. 6: I_0 is the zeroth-order Bessel function of imaginary argument; the characteristic time t_0 and the parameter α are given by

$$\begin{aligned}t_0^{-1} &= [\tfrac{32}{9} s(s+1)]^{2/3} \left(\frac{2\pi D}{c^2 J_0/\hbar}\right)^{-1/3} \\ &\quad\times \left(\frac{J_1}{J_0}\right)^{1/3} \frac{J_1}{\hbar},\end{aligned} \tag{A6}$$

$$\alpha = J_2/J_1,$$

where J_0 is the exchange integral between nearest neighbors in the chain, and J_1 and J_2 the exchange integrals in two directions perpendicular to the chain axis. For the cutoff function (A5), the characteristic frequency may be evaluated by setting

$$\gamma^x_i(\omega_c^{-1}) = e^{-1},$$

so that, for different values of α and for spin $\frac{1}{2}$ and $D \simeq \sqrt{\pi}\,(J_0/\hbar)c^2$ (Ref. 2) the resulting ω_c are given in Table III.

In Ref. 6, to get Eq. (A3), a "decoupling" is proposed which is justified by short-time arguments. It would be valid only for small values of q_x such as $Dq_x^2 \ll \omega_c$. In order to avoid this difficulty, we performed a different derivation, which is presented in Appendix B.

APPENDIX B: CALCULUS OF THE CUTOFF FREQUENCY

In a linear system of spins coupled by Heisenberg interactions E_c, the two-spin correlation function $\tilde{\Gamma}_i(t)$ is expected to display a diffusive behavior,

$$\tilde{\Gamma}_i(t) = \left(\frac{4\pi D}{c^2 J_0/\hbar}\right)^{-1/2} \left(\frac{J_0}{\hbar}\, t\right)^{-1/2} \tag{B1}$$

for $(J_0/\hbar)t \gg 1$.

Different causes can drastically change the linear diffusive behavior. First we consider the influence of small *interchain* interactions E_I on $\Gamma_i^x(t)$:

$$\Gamma_i^x(t) = \langle s_0^x(t) s_i^x(0)\rangle / \langle (s_0^x)^2\rangle \,, \tag{B2}$$

where

$$s_0^x(t) = e^{i(E_c+E_I)t/\hbar}\, s_0^x\, e^{-i(E_c+E_I)t/\hbar} \,.$$

The problem is to describe this function at time t of the order of ω_c^{-1}, ω_c being the cutoff frequency that we assume to be much smaller than $\omega_x = J_0/\hbar$. For this time, $\tilde{\Gamma}_i(t)$ is slowly decreasing in $t^{-1/2}$ as shown by Eq. (B1). The description of the deviation from the linear diffusive behavior may be obtained directly by expanding the operator $s_i^x(t)$ as a function of the perturbation E_c. We define an interaction representation whereby

$$s_0^x(t) = e^{+iE_c t/\hbar}\, \bar{s}_0^x(t)\, e^{-iE_c t/\hbar} \,. \tag{B3}$$

The equation of motion for $\bar{s}_0^x(t)$ is

$$\frac{d}{dt}\, \bar{s}_0^x(t) = \frac{i}{\hbar}\, [E_I(-t), \bar{s}_0^x(t)] \,.$$

After integration, we get

$$\bar{s}_0^x(t) = s_0^x + \frac{i}{\hbar}\int_0^t d\tau\, [\bar{E}_I(-\tau), \bar{s}_0^x(\tau)] \,. \tag{B4}$$

By successive iterations of Eq. (B4) and by using the transformation (B3), the following perturbation expansion is obtained:

$$s_0^x(t) = \tilde{s}_0^x(t) + \frac{i}{\hbar}\int_0^t d\tau\, e^{iE_c t/\hbar}[\bar{E}_I(-\tau), s_0^x] e^{-iE_c t/\hbar} - \frac{1}{\hbar^2}\, e^{iE_c t/\hbar}\int_0^t d\tau \int_0^\tau d\tau' \{\bar{E}_I(-\tau), [\bar{E}_I(-\tau'), s_0^x]\}\, e^{-iE_c t/\hbar} \,. \tag{B5}$$

The first term (of zeroth order) is the operator $\tilde{s}_i^x(t)$, which has a time dependence strictly given by the intrachain Hamiltonian E_c. The terms of higher order come from the perturbation E_I. By setting up (B5) in Eq. (B2) we get

$$\Gamma_i^x(t) \simeq \tilde{\Gamma}_i(t) - \frac{1}{\hbar^2}\int_0^t d\tau \int_0^t d\tau' \langle e^{iE_c(\tau-\tau')/\hbar}[E_I, \tilde{s}_0^x(\tau)]\, e^{-iE_c(\tau-\tau')/\hbar}[\tilde{s}_i^x(-t+\tau'), E_I]\rangle / \langle (s_0^x)^2\rangle \,. \tag{B6}$$

In this expression, we have skipped the first-order term, which at this stage is not zero but which will cancel exactly to zero after we have made the next approximation. In the second term of (B6), the high-temperature limit has been taken into account.

Now we consider that, for $\omega_c t \sim 1$, the motion of any operator $s_i^x(t)$ comes mainly from the components $\tilde{s}_{q_x}(t)$ for small values of the wave vector q_x. The operator s_{q_x} is defined in Appendix A by Eq. (A2) and one has

$$\tilde{s}_{q_x}^x(t) = e^{iE_c t/\hbar}\, s_{q_x}^x\, e^{-iE_c t/\hbar} = s_{q_x}^x + \frac{i}{\hbar}\int_0^t d\tau\, e^{iE_c t/\hbar}[E_c, s_{q_x}^x]\, e^{-iE_c t/\hbar} \,. \tag{B7}$$

For long time t and small values of q_x, $\tilde{s}_q^x(t)$ evolves slowly. In the limit $q_x = 0$, we have exactly

$$\tilde{S}_{(q=0)}^x(t) = S_{(q_x=0)}^x \,,$$

because $s_{(q=0)}^x$ is proportional to the macroscopic spin component $S^x = \sum_{i=1}^N s_i^x$ and $[E, S^x] = 0$. In Eq. (B7) we then keep only the static contribution and in the second-order term of Eq. (B6) we make the approximation to ignore the time dependence of the operators $\tilde{s}_0^x(t)$ and $\tilde{s}_i^x(t)$. The terms neglected are corrections of higher order in the perturbation expansion. We note here that the same approximation is implicitly made in the derivation of Ref. 6. Equation (B6) becomes

$$\Gamma_i^x(t) \simeq \tilde{\Gamma}_i(t) - \frac{1}{\hbar^2}\int_0^t d\tau (t-\tau)$$

TABLE III. Cutoff frequency ω_c as a function of the quantity $(J_1/\hbar)(J_1/J_0)^{1/3}$ for different ratios $\alpha = J_1/J_2$, according to the derivation of Hennessy, McElwee, and Richards (Ref. 6).

α	$\omega_c t_0$	$\omega_c[(J_1/\hbar)(J_1/J_0)^{1/3}]^{-1}$
1	1.7	1.46
0.5	1.25	1.07
$\lesssim 0.3$	1.11	0.96

$$\times \frac{\langle e^{iE_c\tau/\hbar}[E_I, s_0^x]e^{-iE_c\tau/\hbar}[s_i^x, E_I]\rangle}{\langle (s_0^x)^2\rangle} . \quad \text{(B8)}$$

The commutator $[E_I, s_0^x]$ is calculated for the Heisenberg Hamiltonian

$$E_I = \sum_{ij} J_{ij}\vec{s}_i \cdot \vec{s}_j .$$

As in Appendix A, we assume that E_I couples only nearest neighbors. The exchange integrals in two directions perpendicular to the chain are J_1 and J_2. Because of the interchain nature of E_I, the four-spin correlation functions which appear in the second term of (B8) can be changed into products of two-spin correlation functions as $\tilde{\Gamma}_i(t)$ and this gives

$$\Gamma_i^x(t) \simeq \tilde{\Gamma}_i(t) - \tfrac{16}{3}s(s+1)\left(\frac{J_1^2+J_2^2}{\hbar^2}\right) \times \int_0^t d\tau(t-\tau)[\Gamma_i(\tau)]^2 . \quad \text{(B9)}$$

The results of Tahir-Kheli and McFadden for $\tilde{\Gamma}_i(\tau)$, as they are explained in Sec. V, may be used to perform the integration in Eq. (B9). According to the condition

$$1 < \omega_x t < e^{4\pi D\hbar/c^2 J_0} \simeq 10^{10}$$

the integral in (B9) is linearly dependent on time and for the autocorrelation function ($i=0$), it is equal to $\epsilon(J_0/\hbar)^{-1}t$, with $\epsilon = 0.54$ as determined numerically. We then write (B9)

$$\frac{\Gamma_0^x(t)}{\tilde{\Gamma}_0(t)} = \left(1 - \tfrac{16}{3}s(s+1)\frac{(J_1^2+J_2^2)/\hbar^2}{J_0/\hbar}\epsilon\frac{t}{\tilde{\Gamma}_0(t)}\cdots\right) . \quad \text{(B10)}$$

This result gives the cutoff function $\gamma_\epsilon(t)$ defined in Sec. V by Eq. (20). For $\omega_c t \sim 1$, $\tilde{\Gamma}_0(t)$ has the form (B1) and if we compare Eq. (B10) with a development of an exponential function

$$\Gamma_\epsilon^x(t) = e^{-(\omega_c t)^{3/2}} , \quad \text{(B11)}$$

where the cutoff frequency is given by

$$\omega_c = [\tfrac{16}{3}\epsilon s(s+1)]^{2/3}\left(\frac{4\pi D}{c^2 J_0/\hbar}\right)^{1/3} \times (1+\alpha^2)^{2/3}\frac{J_1}{\hbar}\left(\frac{J_1}{J_0}\right)^{1/3} , \quad \text{(B12)}$$

TABLE IV. Cutoff frequency ω_c as a function of the quantity $(J_1/\hbar)(J_1/J_0)^{1/3}$ for different ratios $\alpha = J_1/J_2$, according to the present derivation.

α	$\omega_c[(J_1/\hbar)(J_1/J_0)^{1/3}]^{-1}$
1	7.1
0.5	5.2
$\lesssim 0.3$	4.7

with $\alpha = J_2/J_1$. For $s = \frac{1}{2}$ and $D = \sqrt{\pi}(J_0/\hbar)c^2$, we get the values which are given in Table IV. These values are greater than the results given in Appendix A and Table III. Therefore the present derivation yields a more important cutoff effect.

Our calculation is basically a short-time expansion of the function $\gamma_\epsilon(t)$ and, therefore, its validity is limited to $\omega_c t < 1$. However, it is reasonable to assume that it predicts a correct evaluation of ω_c. If $J_1 \gg J_2$, Eq. (B12) could give the frequency transition from a linear diffusive behavior ($t^{-1/2}$) to a plane diffusive behavior (t^{-1}), the three-dimensional cutoff taking place later. A t^{-1} evolution of $\Gamma_i^x(t)$ would give rise again to a divergence of the spectral density at zero frequency. Therefore, in the case $J_1 \gg J_2$ a different calculation of the cutoff frequency must be performed.

The present derivation may be performed for different correlation functions. The cutoff frequency of the function $\Gamma_0^*(t)$ is still evaluated by (B12). For the first cross-correlation function $\Gamma_i^\alpha(t)$, the characteristic frequency of the cutoff function is

$$\omega_c = [\tfrac{16}{3}\epsilon' s(s+1)]^{2/3}\left(\frac{4\pi D}{c^2 J_0/\hbar}\right)^{1/3} \times (1+\alpha^2)^{2/3}\frac{J_1}{\hbar}\left(\frac{J_1}{J_0}\right)^{1/3} , \quad \text{(B13)}$$

where $\epsilon' = 0.175$ as determined numerically from the integral in (B9), with $i=1$, equal to $\epsilon'(J_0/\hbar)t$.

Let us now examine the role of intrachain interactions $\mathcal{H}_c$. The assumption of a diffusion process requires that, in the chain, the total magnetic flux be conserved. This property is expressed as follows:

$$\frac{d}{dt}\sum_{i=1}^{N}\langle e^{i\mathcal{H}_c t/\hbar}s_i^\alpha e^{-i\mathcal{H}_c t/\hbar}s_0^{\alpha *}\rangle = 0 . \quad \text{(B14)}$$

This fundamental condition is satisfied by the commutation rule

$$[S^\alpha, \mathcal{H}_c] = 0 \quad (\alpha = z, +) . \quad \text{(B15)}$$

If $\mathcal{H}_c$ is only a Heisenberg Hamiltonian, such as

$$E_c = -2J_0\sum_i \vec{s}_i \cdot \vec{s}_{i+1} ,$$

the correlation functions for any component of the spin ($\alpha = z, +$) may be described by a one-dimensional diffusive behavior. This is the case for $\tilde{\Gamma}_i(t)$. If $\mathcal{H}_c$ is not a perfect Heisenberg type and has an extra Ising term

$$\Delta E_c = -2\Delta J_0\sum_i s_i^z s_{i+1}^z \quad \text{(B16)}$$

(where z refers to a direction parallel to the chain), Eq. (B15), with $\mathcal{H}_c = E_c + \Delta E_c$, is true for $\alpha = z$ but

it is not for $\alpha = +$. Thus, the description of $\Gamma_i^z(t)$ by means of a diffusion law ($t^{-1/2}$) remains valid. It is no longer valid for $\Gamma_i^+(t)$. For $\Delta J_0 \ll J_0$ we can again evaluate the deviation from the "ideal" Heisenberg chain by considering ΔE_c as a perturbation term. The derivation is the same and we arrive at an equation like (B10), which, for the autocorrelation function, is

$$\Gamma_0^+(t) \simeq \tilde{\Gamma}_i(t) - \tfrac{8}{3} s(s+1) \left(\frac{\Delta J_0}{\hbar}\right)^2 \times \int_0^t d\tau (t-\tau) \tilde{\gamma}_0^{(4)}(\tau) , \quad \text{(B17)}$$

where

$$\tilde{\gamma}_0^{(4)}(\tau) = \frac{\langle e^{iE_c t/\hbar} s_0^+ s_1^z e^{-iE_c t/\hbar} s_0^- s_1^z \rangle}{\langle s_0^+ s_0^- (s_1^z)^2 \rangle} \quad \text{(B18)}$$

is a four-spin correlation function, the spins s_i and s_{i+1} being located on the same chain. We note here that such a term as the second one in Eq. (B17) appears in the Kubo-Tomita (KT) formalism of the resonance line shape.[8] In order to explain the non-Lorentzian shape of the electronic-paramagnetic-resonance (EPR) line in some one-dimensional Heisenberg systems, different authors[4,6,7] have given the four-spin correlation function $\tilde{\gamma}_0^{(4)}(t)$ a diffusive behavior, as the two-spin correlation function $\tilde{\Gamma}_i(t)$ has. However, the KT formalism, like the present derivation, is basically a short-time expansion, and for this reason it can only be used to interpret pure-Lorentzian shape. In Tanol, the EPR line shape is purely Lorentzian to at least four linewidths for any direction of the magnetic field.[34] Consequently, the function $\tilde{\gamma}_0^{(4)}(t)$ must be supposed to have an internal cutoff which limits its evolution at times much shorter than T_2, the inverse of the linewidth. Therefore, the usual approximations of the KT description can be repeated, neglecting τ compared to t and replacing t by infinity in the integral of Eq. (B17), which is still linearly dependent on time. Then, as in the previous study, the cutoff function is given by Eq. (B11) and the cutoff frequency is

$$\omega_c = \left(\tfrac{4}{3} s(s+1) 2\pi \frac{J_0}{\hbar} \phi_0^{(4)}(\omega = 0)\right)^{2/3} \times \left(\frac{4\pi D}{c^2 J_0/\hbar}\right)^{1/3} \left(\frac{\Delta J_0}{J_0}\right)^{1/3} \frac{\Delta J_0}{\hbar} , \quad \text{(B19)}$$

where $\phi_0^{(4)}(\omega)$ is the Fourier transform of $\tilde{\gamma}_0^{(4)}(t)$ [Eq. (B18)].

In a similar way, the intrachain dipolar interactions lead to cutoff effects. The secular term

$$d_0 = \tfrac{3}{2}(1 - 3\cos^2\theta) \sum_{i<j} \frac{\hbar^2 \gamma_e^2}{r_{ij}^3} s_i^z s_j^z \quad \text{(B20)}$$

has the same form as (B16) and therefore it gives a cutoff to $\Gamma_i^+(t)$. In Eq. (B20), θ is the angle between the external magnetic field H_0 and the chain direction, and r_{ij} is the distance between two spins of the chain. In this case the cutoff frequency is angularly dependent:

$$\omega_c = \left(\tfrac{3}{4} s(s+1) 2\pi \frac{J_0}{\hbar} \phi_0^{(4)}(\omega = 0)(1 - 3\cos^2\theta)^2\right)^{2/3} \times \left(\frac{4\pi D}{c^2 J_0/\hbar}\right)^{1/3} \left(\frac{\hbar\gamma_e^2/c^3}{J_0/\hbar}\right)^{1/3} \left(\frac{\hbar\gamma_e^2}{c^3}\right) . \quad \text{(B21)}$$

The nonsecular terms

$$d_{\pm 1} = -\tfrac{3}{2} \sin\theta \cos\theta \, e^{\mp i\phi} \sum_{i<j} \frac{\hbar\gamma_e^2}{r_{ij}^3} (s_i^z s_j^\pm + s_i^\pm s_j^z)$$

and

$$d_{\pm 2} = \tfrac{3}{4} \sin^2\theta \, e^{\mp 2i\phi} \sum_{i<j} \frac{\hbar\gamma_e^2}{r_{ij}^3} s_i^\pm s_j^\pm$$

give rise to cutoff effects on both $\Gamma_i^z(t)$ and $\Gamma_i^+(t)$. The cutoff frequencies are now functions of the electronic Larmor frequency, $\omega_e = \gamma_e \hbar H_0$:

$$\omega_c = \left(\tfrac{9}{2} s(s+1) 2\pi \frac{J_0}{\hbar} \phi_0^{(4)}(\omega_e) \sin^2\theta \cos^2\theta + \tfrac{3}{4} s(s+1) 2\pi \frac{J_0}{\hbar} \phi_0^{(4)}(2\omega_e) \sin^4\theta\right)^{2/3} \times \left(\frac{4\pi D}{c^2 J_0/\hbar}\right)^{1/3} \left(\frac{\hbar\gamma_e^2/c^3}{J_0/\hbar}\right)^{1/3} \left(\frac{\hbar\gamma_e^2}{c^3}\right) \quad \text{(B22)}$$

for the function $\Gamma_0^+(t)$ and

$$\omega_c = \left(3 s(s+1) 2\pi \frac{J_0}{\hbar} \phi_0^{(4)}(\omega_e) \sin^2\theta \cos^2\theta + 3 s(s+1) \frac{2\pi J_0}{\hbar} \phi_0^{(4)}(2\omega_e) \sin^4\theta\right)^{2/3} \times \left(\frac{4\pi D}{c^2 J_0/\hbar}\right)^{1/3} \left(\frac{\hbar\gamma_e^2/c^3}{J_0/\hbar}\right)^{1/3} \left(\frac{\hbar\gamma_e^2}{c^3}\right) \quad \text{(B23)}$$

for the function $\Gamma_0^z(t)$.

By comparison with the EPR linewidth, we can get a phenomenological evaluation of ω_c. For this, let us assume that only the intrachain dipolar interaction contributes to the linewidth ΔH. (This is not exactly true in Tanol where the anisotropy of ΔH shows that the contribution of the interchain dipolar interactions are not negligible.[34]) In this approximation and because the EPR line shape is Lorentzian, the linewidth is given in the KT formalism by the expression

$$\delta = \left(\tfrac{3}{4} s(s+1) 2\pi \frac{J_0}{\hbar} \phi_0^{(4)}(\omega = 0)(1 - 3\cos^2\theta)^2 + \tfrac{9}{2} s(s+1) 2\pi \frac{J_0}{\hbar} \phi_0^{(4)}(\omega_e) \sin^2\theta \cos^2\theta + \tfrac{3}{4} s(s+1) \frac{2\pi J_0}{\hbar} \phi_0^{(4)}(2\omega_e) \sin^4\theta\right) \frac{\hbar\gamma_e^2/c^3}{J_0/\hbar} \frac{\hbar\gamma_e}{c^3} . \quad \text{(B24)}$$

Then combining (B21), (B22), and (B24) we get

$$\omega_c = \left(\frac{4\pi D}{c^2 J_0/\hbar}\right)^{1/3} \left(\frac{\hbar\gamma_e^2/c^3}{J_0/\hbar}\right)^{-1/3} \left(\frac{\delta}{\hbar\gamma_e^2/c^3}\right)^{-1/3} \delta \ . \tag{B25}$$

This formula must be considered as an upper bound of the cutoff frequency ω_c in $\Gamma_0^x(t)$ due to all the intrachain dipolar terms. In Tanol, the largest value of the linewidth observed in a field $H_0 = 2000$ Oe is $\Delta H = 3$ Oe.[34] Therefore from (B24) we get

$$\omega_c/k < 0.026 \text{ K} \ .$$

[1]F. Carboni and P. M. Richards, Phys. Rev. 177, 889 (1969).
[2]R. A. Tahir-Kheli and D. G. McFadden, Phys. Rev. 182, 604 (1969).
[3]F. B. McLean and M. Blume, Phys. Rev. B 7, 1149 (1973).
[4]R. N. Rogers, F. Carboni, and P. M. Richards, Phys. Rev. Lett. 19, 1016 (1967).
[5]R. E. Dietz, F. R. Meritt, R. Dingle, D. Hone, B. G. Silbernagel, and P. M. Richards, Phys. Rev. Lett. 26, 1186 (1971).
[6]M. J. Hennessy, C. D. McElwee, and P. M. Richards, Phys. Rev. B 7, 930 (1973).
[7]R. R. Barthowski, M. J. Hennessy, B. Morosin, and P. Richards, Solid State Commun. 11, 405 (1972); R. R. Barthowski and B. Morosin, Phys. Rev. B 6, 4209 (1972); K. Okuda, H. Hoto, and M. Date, J. Phys. Soc. Jap. 33, 1574 (1972).
[8]R. Kubo and Tomita, J. Phys. Soc. Jap. 9, 888 (1954).
[9]S. M. Myers and A. Narath, Phys. Rev. Lett. 27, 641 (1971).
[10]D. W. Hone and B. G. Silbernagel, J. Phys. (Paris) 32, C1 (1971); J. E. Gulley, D. Hone, D. J. Scalapino, and B. G. Silbernagel, Phys. Rev. B 1, 1020 (1970).
[11]J.-P. Boucher and M. Nechtschein, J. Phys. (Paris) 31, 783 (1970).
[12]J.-P. Boucher, thesis (Grenoble, 1972)(unpublished).
[13]J.-P. Boucher and H. Jouve, Phys. Lett. 34, 229 (1971).
[14]Y. Barjhoux *et al.* (unpublished).
[15]J. Lajzerowicz-Bonneteau, Acta Crystallogr. B 24, 196 (1968).
[16]L. J. Berliner, Acta Crystallogr. B 26, 1198 (1970).
[17]F. Ferrieu and M. Nechtschein, Chem. Phys. Lett. 11, 46 (1971).
[18]R. Briere, H. Lemaire, A. Rassat, and J. J. Dunand, Bull. Soc. Chim. Fr. 4220 (1970).
[19]H. Lemaire, P. Rey, A. Rassat, A. De Combarieu, and J. C. Michel, Mol. Phys. 14, 201 (1968).
[20]J. C. Bonner and M. E. Fisher, Phys. Rev. 135, A640 (1964).
[21]C. Veyret and A. Blaise, Mol. Phys. 25, 873 (1973).
[22]J.-P. Boucher, M. Nechtschein, and M. Saint Paul, Phys. Lett. A 42, 397 (1973).
[23]H. Jouve, thesis (Grenoble, 1970) (unpublished).
[24]J.-P. Boucher, H. Jouve, and M. Nechtschein, J. Mag. Resonance 6, 396 (1972).
[25]M. Nechtschein, H. Jouve, F. Ferrieu, and J.-P. Boucher, Phys. Lett. A 36, 347 (1971). An error occurred in the calculation of the theoretical curve which is given in this letter. Correct curve is given in Ref. 24.
[26]J.-P. Boucher, F. Ferrieu, and M. Nechtschein, in *Proceedings of the Seventeenth Colloque Ampère, Turku*, 1972, edited by V. Hovi (North-Holland, Amsterdam, 1973), p. 369.
[27]T. Oguchi, Phys. Rev. 133, A1098 (1964).
[28]R. A. Tahir-Kheli, Phys. Rev. 132, 689 (1963).
[29]T. Moriya, Phys. Rev. 120, 91 (1960); J. H. Van Vleck, J. Phys. Radium 12, 262 (1951).
[30]H. Lemaire, thesis (Grenoble, 1966)(unpublished).
[31]P. G. De Gennes, J. Phys. Chem. Solids 4, 223 (1958).
[32]C. D. Mc Elwee, thesis (University of Kansas, 1970) (unpublished).
[33]C. Veyret (private communication).
[34]H. Lemaire (private communication).